Reduction of (18)F-FDG Dose in Clinical PET/MR Imaging by Using Silicon Photomultiplier Detectors

Sekine, Tetsuro ; Delso, Gaspar ; Zeimpekis, Konstantinos G ; de Galiza Barbosa, Felipe ; ter Voert, Edwin E G W ; Huellner, Martin ; Veit-Haibach, Patrick

Abstract: Purpose To determine the level of clinically acceptable reduction in injected fluorine 18 ((18)F) fluorodeoxyglucose (FDG) dose in time-of-flight (TOF)-positron emission tomography(PET)/magnetic resonance (MR) imaging by using silicon photomultiplier (SiPM) detectors compared with TOF-PET/computed tomography (CT) using Lu1.8Y0.2SiO5(Ce), or LYSO, detectors in patients with different body mass indexes (BMIs). Materials and Methods Patients were enrolled in this study as part of a larger prospective study with a different purpose than evaluated in this study (NCT02316431). All patients gave written informed consent prior to inclusion into the study. In this study, 74 patients with different malignant diseases underwent sequential whole-body TOF-PET/CT and TOF-PET/MR imaging. PET images with simulated reduction of injected (18)F-FDG doses were generated by unlisting the list-mode data from PET/MR imaging. Two readers rated the image quality of whole-body data sets, as well as the image quality in each body compartment, and evaluated the conspicuity of malignant lesions. Results The image quality with 70% or 60% of the injected dose of (18)F-FDG at PET/MR imaging was comparable to that at PET/CT. With 50% of the injected dose, comparable image quality was maintained among patients with a BMI of less than 25 kg/m(2). PET images without TOF reconstruction showed higher artifact scores and deteriorated sharpness than those with TOF reconstruction. Conclusion Sixty percent of the usually injected (18)F-FDG dose (reduction of up to 40%) in patients with a BMI of more than 25 kg/m(2) results in clinically adequate PET image quality in TOF-PET/MR imaging performed by using SiPM detectors. Additionally, in patients with a BMI of less than 25 kg/m(2), 50% of the injected dose may safely be used. (©) RSNA, 2017 Online supplemental material is available for this article.

DOI: https://doi.org/10.1148/radiol.2017162305

Radiology

Reduction of ^{18}F-FDG Dose in Clinical PET/MR Imaging by Using Silicon Photomultiplier Detectors[1]

Tetsuro Sekine, MD, PhD[2]
Gaspar Delso, PhD
Konstantinos G. Zeimpekis, MS
Felipe de Galiza Barbosa, MD
Edwin E. G. W. ter Voert, MS
Martin Huellner, MD
Patrick Veit-Haibach, MD

Purpose: To determine the level of clinically acceptable reduction in injected fluorine 18 (^{18}F) fluorodeoxyglucose (FDG) dose in time-of-flight (TOF)–positron emission tomography(PET)/magnetic resonance (MR) imaging by using silicon photomultiplier (SiPM) detectors compared with TOF-PET/computed tomography (CT) using $Lu1.8Y0.2SiO_5(Ce)$, or LYSO, detectors in patients with different body mass indexes (BMIs).

Materials and Methods: Patients were enrolled in this study as part of a larger prospective study with a different purpose than evaluated in this study (NCT02316431). All patients gave written informed consent prior to inclusion into the study. In this study, 74 patients with different malignant diseases underwent sequential whole-body TOF-PET/CT and TOF-PET/MR imaging. PET images with simulated reduction of injected ^{18}F-FDG doses were generated by unlisting the list-mode data from PET/MR imaging. Two readers rated the image quality of whole-body data sets, as well as the image quality in each body compartment, and evaluated the conspicuity of malignant lesions.

Results: The image quality with 70% or 60% of the injected dose of ^{18}F-FDG at PET/MR imaging was comparable to that at PET/CT. With 50% of the injected dose, comparable image quality was maintained among patients with a BMI of less than 25 kg/m^2. PET images without TOF reconstruction showed higher artifact scores and deteriorated sharpness than those with TOF reconstruction.

Conclusion: Sixty percent of the usually injected ^{18}F-FDG dose (reduction of up to 40%) in patients with a BMI of more than 25 kg/m^2 results in clinically adequate PET image quality in TOF-PET/MR imaging performed by using SiPM detectors. Additionally, in patients with a BMI of less than 25 kg/m^2, 50% of the injected dose may safely be used.

Online supplemental material is available for this article.

[1] From the Departments of Nuclear Medicine (T.S., K.G.Z., F.d.G.B., E.E.G.W.t.V., M.H., P.V.), Neuroradiology (M.H.), and Diagnostic and Interventional Radiology (P.V.), University Hospital Zurich, Ramistrasse 100, 8091 Zurich, Switzerland; Department of Radiology, Nippon Medical School, Tokyo, Japan (T.S.); Applied Science Laboratory, GE Healthcare, Waukesha, Wis (G.D.); and University of Zurich, Zurich, Switzerland (E.E.G.W.t.V., M.H., P.V.). Received October 31, 2016; revision requested December 21; revision received May 1, 2017; accepted June 5; final version accepted June 8. **Address correspondence to** T.S. (e-mail: *tetsuro.sekine@gmail.com*).

Positron emission tomography (PET)/computed tomography (CT) is widely used for the assessment of tumor stage and therapy response (1,2). The CT component is used both for attenuation correction and for anatomic correlation and characterization of lesions with pathologic radiotracer uptake (3).

Advances in Knowledge

- Silicon photomultiplier (SiPM) detectors, which enable time-of-flight (TOF)-PET in PET/MR imaging systems, are more sensitive than the Lu1.8Y0.2 SiO_5(Ce) (LYSO) crystals in conventional TOF-PET/CT; the increased sensitivity of SiPMs can be used to lower the injected dose of radioactive tracers.
- PET image quality with simulated 60% of the standard injected dose (reduction of up to 40%) at TOF-PET/MR imaging with SiPM detectors was found to be comparable to that at standard TOF-PET/CT with LYSO detectors.
- When 50% of the standard injected dose was used (reduction of up to 50%) in TOF-PET/MR imaging with SiPM, there were significant differences in image quality of maximum intensity projections (MIPs), sharpness, and noise among the four body mass index (BMI) groups (MIP, sharpness in chest and noise in pelvist, $P < .05$; noise in chest and upper abdomen, $P < .01$), resulting in acceptable imaging quality in the BMI of less than 25 kg/m^2 group and unacceptable imaging quality in the BMI of more than 25 kg/m^2 group.
- Even when 40% of the standard injected dose was used (reduction of up to 60%), no lesions were missed on PET images with TOF reconstruction at PET/MR imaging, while with use of 40% of the injected dose without TOF reconstruction, 12 of 138 lesions were not safely detected.

Despite being one of the most widely used imaging modalities in oncologic imaging, PET/CT results in considerable medical radiation exposure (up to 25 mSv in older systems, and approximately 7–10 mSv at modern state-of-the-art CT), which is somewhat higher than in multidetector contrast material–enhanced CT (depending on the examination protocol) (3,4). Thus, especially for young patients who potentially require repeated follow-up studies, the imaging modality with the lowest possible absorbed radiation dose per examination is desired.

The newly available PET/magnetic resonance (MR) imaging systems can help reduce the absorbed radiation dose to patients (5–7). In these systems, the MR imaging component, which does not require the use of ionizing radiation, replaces the CT component for attenuation correction, anatomic correlation, and diagnostic lesion characterization. Additionally, the PET component from the latest clinical time-of-flight (TOF)-PET/MR imaging systems has the potential to reduce radiation exposure even further. This system uses dedicated silicon photomultiplier (SiPM) detectors with increased sensitivity, which allows one to balance reduction of injected dose with acquisition time reduction (5,8,9). In a pilot study, PET image quality with this system was clinically acceptable at 50% of the injected fluorodeoxyglucose (FDG) dose used in conventional PET/CT (5). However, in that study, only initial results were presented, the imaging quality of malignant lesions was not assessed, and image evaluation was not adapted to body mass index (BMI). Thus, the goal of our study was to determine the level of clinically acceptable reduction of injected fluorine 18 (^{18}F)-FDG dose in TOF-PET/MR imaging using SiPM detectors compared with PET/CT in patients with different BMIs.

Implication for Patient Care

- In PET scans with SiPM technology, 60% of the injected dose (40% dose reduction) of fluorine 18 (^{18}F)-fluorodeoxyglucose (FDG) in patients with a BMI of more than 25 kg/m^2 yields adequate PET image quality in TOF PET/MR imaging, and in patients with a BMI of less than 25 kg/m^2, adequate image quality can be obtained with an ^{18}F-FDG dose reduction of 50%.

Materials and Methods

Patients were enrolled in this retrospective study as a secondary study of a larger prospective study with a different purpose than our study (NCT02316431). All patients gave written informed consent prior to inclusion into the study. Thus, the analysis presented here is based on a retrospective review of prospectively acquired data.

There was financial support for this study from GE Healthcare on an institutional level. GE Healthcare employees participated in this study as authors. Only non–GE Healthcare employees had control of inclusion of the data and information that might present a

https://doi.org/10.1148/radiol.2017162305

Content code: NM

Radiology 2017; 000:1–11

Abbreviations:
BMI = body mass index
FDG = fluorodeoxyglucose
FOV = field of view
LAVA Flex = liver acquisition with volume acquisition
LYSO = Lu1.8Y0.2 SiO_5(Ce)
MIP = maximum intensity projection
OSEM = ordered subset expectation maximization
PSF = point spread function
SiPM = silicon photomultiplier
3D = three-dimensional
TOF = time of flight

Author contributions:
Guarantors of integrity of entire study, T.S., P.V.; study concepts/study design or data acquisition or data analysis/interpretation, all authors; manuscript drafting or manuscript revision for important intellectual content, all authors; manuscript final version approval, all authors; agrees to ensure any questions related to the work are appropriately resolved, all authors; literature research, T.S., K.G.Z., F.d.G.B., M.H., P.V.; clinical studies, T.S., F.d.G.B., M.H.; experimental studies, T.S., G.D.; statistical analysis, T.S.; and manuscript editing, T.S., G.D., K.G.Z., M.H., P.V.

Conflicts of interest are listed at the end of this article.

Table 1

Patient Characteristics

Parameter	Total	BMI < 20 kg/m^2	BMI 20–25 kg/m^2	BMI 25–30 kg/m^2	BMI > 30 kg/m^2
No. of patients	74	10	26	25	13
Sex					
Male	45	3	16	18	8
Female	29	7	10	7	5
Median height (m)	1.72 (1.48–1.90)	1.70 (1.49–1.82)	1.73 (1.49–1.90)	1.70 (1.48–1.90)	1.75 (1.60–1.87)
Median weight (kg)	74 (42–116)	56 (42–63)	69 (54–90)	75 (56–96)	95 (75–116)
Mean patient age (y)	61.4 (29–84)	57.2 (40–74)	62.0 (29–80)	61.0 (31–80)	64.4 (46–84)
Male patients	61.2 (31–80)	51.0 (47–55)	62.8 (50–80)	60.8 (31–80)	62.9 (46–77)
Female patients	61.6 (29–84)	59.9 (40–74)	60.8 (29–79)	61.6 (48–72)	65.6 (55–84)
Tumor type					
Head and neck cancer	18	4	8	6	
Breast cancer	2	1		1	
Lung cancer	11	1	6	4	
Esophageal cancer	4		1	2	1
Gastric cancer	1		1		
Colon cancer	7	1	2	3	1
Cholangiocarcinoma	2	1		1	
Pancreatic cancer	4		1		3
Splenic cancer	1			1	
Multiple myeloma	5	1	1	1	2
Malignant melanoma	4	1	1	2	
Malignant lymphoma	7		2	3	2
Unknown primary tumor	8		3	1	4
Median injected tracer activity (kBq)	219.5 (177.6–337.5)	186.7 (177.9–212.4)	209.1 (177.6–323.1)	225.0 (180–319.1)	321.1 (221.4–337.5)
Median PET/CT postinjection time (min)	72 (46–104)	72 (46–90)	70 (55–100)	76 (57–104)	73 (60–90)
Median PET/MR postinjection time (min)	77 (37–148)	72 (41–125)	89 (38–144)	60 (42–148)	56 (37–129)

Note.—Data in parentheses are ranges. There was no significant difference in postinjection time between PET/CT and PET/MR imaging in all patients (P = .167).

conflict of interest for those authors who are employees of GE Healthcare.

Patients

For inclusion in our study, patients had to meet the following criteria: referral for initial staging or follow-up of a malignant disease between January 2014 and June 2015 in our institution and willingness to undergo the whole-body PET/MR imaging examination in addition to the clinically indicated PET/CT examination. Exclusion criteria were contraindications to MR imaging, such as electronically active implanted medical devices, metallic foreign bodies in sensitive anatomic areas (eg, orbita), severe claustrophobia, or a body size that did not fit into the PET/MR gantry. Patients were classified into four groups according to their BMI (< 20, > 20 to 25, > 25 to 30, or > 30 kg/m^2). Detailed patient information and times from injection to imaging for PET/MR imaging and PET/CT are given in Table 1.

Imaging Examination and Reconstruction

Detailed information on the technical acquisition parameters of PET/CT and PET/MR imaging is given in Table 2.

PET/CT Examination

The PET/CT acquisition followed a standard protocol for clinical oncologic imaging on a TOF PET/CT scanner (Discovery 690; GE Healthcare, Waukesha, Wis) (5,6).

First, a helical CT acquisition was performed for attenuation correction of PET data. The scan parameters were as follows: 120 kVp; 15–80 mA with automatic dose modulation; rotation time, 0.5 second; helical thickness, 3.75 mm; pitch, 39.37 mm per rotation; matrix size, 512 × 512 pixels; section thickness, 3.3 mm; and pixel size, 1.4 × 1.4 mm^2. Then, whole-body PET data were acquired in 3D TOF mode with a scan duration of 2 minutes per bed position, an axial FOV of 153 mm, and 23% overlap of bed positions, resulting in a total PET acquisition time of 16–20 minutes (11).

PET/MR Imaging Examination

PET/CT and PET/MR imaging were performed with one radionuclide injection. For the PET/MR imaging examination, we used a simultaneous PET/MR system, which comprises 3.0-T whole-body MR imaging and SiPM PET detectors (SIGNA PET/MR; GE Healthcare) (12).

Whole-body list-mode PET data were acquired in 3D TOF mode with a scan duration of 2–4 minutes per bed position. The scan time per bed position

Table 2

Technical Acquisition Parameters of PET/CT and PET/MR Imaging

Parameter	PET/CT	PET/MR
Crystal type	LYSO	SiPM
Crystal size (mm)	4.2 × 6.3 × 25	3.95 × 5.3 × 25
Timing resolution (psec)	544	385
PET transaxial FOV (mm)	810	622
PET axial FOV (mm)	157	250
Overlap between beds (%)	23	24
Scan duration per bed	2 min	2–4-min retrospective unlisting
Total bed acquisition	8–10	6
Attenuation correction	CT	Dixon MR imaging (4-class)
Reconstruction	3D-OSEM	3D-OSEM
TOF	On	On and off
PSF	On	On
Scatter correction	On	On
Iterations	3	3
Subsets	18	16
Voxel size (mm)	2.73 × 2.73 × 3.27	2.34 × 2.34 × 2.78

Note.—FOV = field of view, LYSO = $Lu1.8Y0.2 SiO_5(Ce)$, OSEM = ordered subset expectation maximization, PSF = point spread function, 3D = three-dimensional. See also reference 10.

depended on the imaging protocol selected according to the clinical indication. An axial FOV of 250 mm and 24% overlap of bed positions were used, resulting in a total PET acquisition time of 12–24 minutes. During PET/MR imaging, a 3D liver acquisition with volume acquisition (LAVA Flex) T1-weighted pulse sequence (repetition time, approximately 4 msec; echo time, 2.23 msec; flip angle, 5°; section thickness, 5.2 mm with 2.6 mm overlap; 120 sections; pixel size, 1.95 × 1.95 mm^2, partial Fourier 70.3%; and acquisition time, 18 seconds per bed position) for MR imaging–based attenuation correction was performed. Additionally, different anatomic MR pulse sequences for diagnostic imaging were also performed (13).

General PET Reconstruction Parameters

PET images from PET/CT and from PET/MR imaging were reconstructed by using parameters that were as similar as possible. In PET/CT, a fully 3D OSEM iterative reconstruction, including PSF compensation with three iterations and 18 subsets and a 256 × 256 image grid (2.73 × 2.73 × 3.27-mm voxels), was used.

In PET/MR imaging, OSEM, including PSF compensation with three iterations and 16 subsets and a 256 × 256 image grid (2.34 × 2.34 × 2.78-mm voxels), was used for reconstruction of the PET images.

The difference in voxel size is due to differences in crystal size and FOV. Images were filtered in image space by using a 4-mm full width at half maximum in-plane Gaussian filter, followed by an axial filter with a three-section kernel using relative weights of 1:4:1. Scatter correction was applied. For PET/MR imging, truncation completion was performed by using non–attenuation-corrected PET images. Attenuation correction was accomplished by using the CT data at PET/CT and the LAVA Flex T1-weighted data at PET/MR imaging (12). Clinical PET data derived from PET/CT were generated by TOF calculation from emission data and were defined as the standard of reference for the evaluation and comparison with PET images derived from PET/MR imaging. PET images with simulated reduced injected ^{18}F-FDG doses with and without TOF were obtained from emission data from PET/MR imaging by retrospectively unlisting the list-mode data, as described in the next paragraph.

PET Images with Simulated Reduced Injected ^{18}F-FDG Doses at PET/MR Imaging

To obtain PET images with simulated reduced injected ^{18}F-FDG doses, eight sets of PET images were reconstructed from identical PET emission data from the PET/MR acquisition in each patient. We retrospectively unlisted the list-mode data in the PET images derived from PET/MR imaging to obtain a reduced amount of emitted counts, equivalent to 70%, 60%, 50%, and 40% of counts compared with PET images derived from PET/CT (hereafter, $^{70\%}$PET, $^{60\%}$PET, $^{50\%}$PET, and $^{40\%}$PET). These four sets of simulated reduced doses were chosen on the basis of the results from a preliminary study (5). For this adjustment, the radioactive decay between the acquisition of PET/CT and PET/MR data was taken into account. In addition, PET image sets were recontructed with TOF and without TOF (hereafter, PET_{TOF} and $PET_{non\text{-}TOF}$), which resulted in a total of eight reconstructed PET image data sets (eg, $^{70\%}PET_{TOF,}$ $^{70\%}PET_{non\text{-}TOF}$).

The signal-to-noise ratio of PET images was determined according to a Poisson counting process (14,15). In this situation, signal-to-noise ratio (SNR) can be expressed as follows:

$$SNR^2 = NECR\ \Delta t\ ,$$

where NECR is noise equivalent count rate. For the range of simulated reduced ^{18}F-FDG doses used in clinical practice, the noise equivalent count rate curve is approximately linear. The image quality of simulated dose-reduced PET images can therefore be approximated by reconstructing a fraction of the measured counts at full dose.

On the basis of this assumption, we created simulated dose-reduced images by unlisting the PET data and reconstructing them based on the percentage of used counts (eg, the PET images were reconstructed from 2-minute list-mode PET data into a 1-minute acquisition, which is similar to 50% of the injected

Figure 1

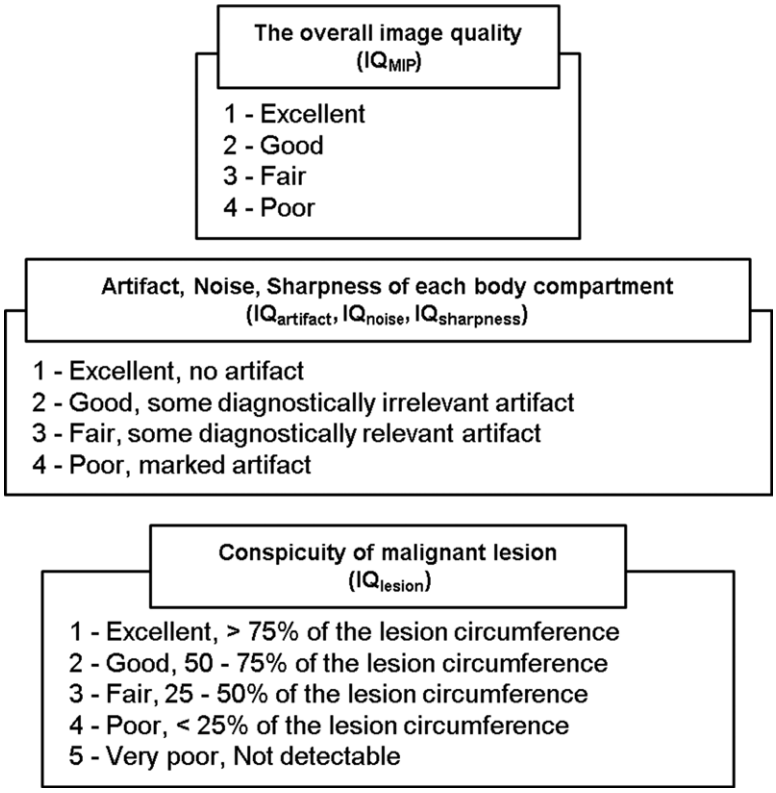

Figure 1: Image quality *(IQ)* parameters. Overall, we classified a score of 1 as indicating that the image quality of simulated PET images was superior or comparable to the standard of reference and a score of 2 as indicating that the image quality of simulated PET images was comparable or very slightly inferior to the standard of reference; therefore, both scores indicated that the images were valid for clinical imaging. *MIP* = maximum intensity projection.

dose) (14,16). All image reconstructions were performed for all patients in all BMI groups.

Image Evaluation

Two radiologists (F.d.G.B. and T.S., with 8 and 11 years of experience in PET reading, respectively) analyzed the images in random order. Both readers were blinded to the reconstructed set and to the simulated injected ^{18}F-FDG dose.

For image evaluation, a dedicated review workstation was used (Advantage Workstation, version 4.6; GE Healthcare, Waukesha, Wis). The clinical TOF-PET images from standard PET/CT were defined as the standard of reference. Readers assessed the eight PET image sets (derived from PET/MR) of simulated dose-reduced images compared with the standard of reference. Analysis of image quality was performed in three steps (Fig 1). First, the overall image quality of the whole-body PET with MIP (IQ_{MIP}) was assessed. Here, a four-point scale was used (ranging from a score of 1 [good] to a score of 4 [not acceptable for diagnosis]). Then, images were assessed with regard to artifacts, noise, and sharpness in different body compartments (head and neck [HN], chest [CH], upper abdomen [UA], and pelvis [PE] [eg, $IQ_{CH\_artifact}$, $IQ_{PE\_sharpness}$]) by using the same four-point scale. Third, the conspicuity of malignant target lesions (IQ_{lesion}) was noted. For the IQ_{lesion}, we used a five-point scale where a score of 1 meant detection of more than 75% of the circumference of the lesion and a score of 5 meant that no lesion was detected. To summarize for clinical applicability, we classified simulated PET images with a score of 1 as superior or comparable to the standard of reference and those with a score of 2 as comparable or slightly inferior to the standard of reference; both summed scores were therefore considered to indicate that the images were adequate for clinical imaging. Detailed image quality parameters are shown in Figure 1.

The target lesions were extracted by the two readers in consensus 3 months before the image evaluation. A maximum of three FDG-avid lesions per body-part compartment (three lesions × four compartments = 12 lesions per patient) were extracted from clinical TOF-PET/CT data. Of those three lesions, one was the smallest lesion and one was the biggest malignant lesion per body compartment. Overall, 138 lesions were evaluated (mean long-axis diameter, 20 mm ± 18).

The assessment of image quality of the PET images with simulated reduced ^{18}F-FDG doses derived from PET/MR imaging was performed in comparison with the standard of reference (clinical TOF-PET images derived from PET/CT).

Statistical Analysis

To compare the agreement between the two readers, we assessed the agreement in all scores by calculating the linear-weighted κ. Agreement was defined as moderate (κ = 0.41–0.60), substantial (κ = 0.61–0.80), or significant (κ > 0.80) (17).

Each of the eight simulated PET image data sets was classified on the basis of the BMI of the patient into four subgroups. To estimate the effect of BMI on the result of our scoring, we performed a one-way analysis of variance (Kruskal-Wallis test) among four BMI groups in a total of 13 categories (MIP and three categories [noise, sharpness and artifact] × four body parts [head and neck, chest, upper abdomen, and pelvis] = 12 categories). We considered clinical and diagnostic quality to be insufficient if more than one of the 13 image quality category scores were higher than 2 in more than 10% of each patient group.

Table 3

Image Quality Score of TOF-PET/MR Imaging with SiPM Detectors in All Patients (n = 74)

Parameter	TOF = On				TOF = Off			
	$^{70\%}PET_{TOF}$	$^{60\%}PET_{TOF}$	$^{50\%}PET_{TOF}$	$^{40\%}PET_{TOF}$	$^{70\%}PET_{non\text{-}TOF}$	$^{60\%}PET_{non\text{-}TOF}$	$^{50\%}PET_{non\text{-}TOF}$	$^{40\%}PET_{non\text{-}TOF}$
Whole-body MIP	1.05 ± 0.21	1.08 ± 0.25	1.43 ± 0.48	1.97 ± 0.47	1.05 ± 0.21	1.08 ± 0.23	1.31 ± 0.37	1.68 ± 0.40
Body compartments								
Head and neck								
Artifact	1.47 ± 0.35	1.47 ± 0.36	1.48 ± 0.36	1.56 ± 0.39	1.76 ± 0.50	1.76 ± 0.48	1.82 ± 0.46	1.85 ± 0.46
Noise	1.03 ± 0.15	1.03 ± 0.14	1.30 ± 0.34	1.84 ± 0.31	1.01 ± 0.09	1.02 ± 0.10	1.26 ± 0.29	1.68 ± 0.33
Sharpness	1.01 ± 0.06	1.01 ± 0.08	1.07 ± 0.17	1.18 ± 0.27	1.64 ± 0.33	1.71 ± 0.30	1.81 ± 0.27	1.89 ± 0.32
Chest								
Artifact	1.04 ± 0.19	1.04 ± 0.18	1.05 ± 0.19	1.14 ± 0.25	1.41 ± 0.50	1.45 ± 0.49	1.50 ± 0.52	1.57 ± 0.52
Noise	1.10 ± 0.26	1.16 ± 0.30	1.71 ± 0.46	2.16 ± 0.41	1.13 ± 0.34	1.15 ± 0.34	1.48 ± 0.41	1.87 ± 0.44
Sharpness	1.05 ± 0.20	1.08 ± 0.26	1.22 ± 0.33	1.57 ± 0.47	1.91 ± 0.30	2.06 ± 0.31	2.23 ± 0.40	2.51 ± 0.41
Upper abdomen								
Artifact	1.04 ± 0.19	1.04 ± 0.18	1.05 ± 0.19	1.14 ± 0.25	1.55 ± 0.51	1.58 ± 0.51	1.64 ± 0.54	1.69 ± 0.51
Noise	1.07 ± 0.21	1.12 ± 0.27	1.59 ± 0.45	2.07 ± 0.37	1.07 ± 0.22	1.17 ± 0.30	1.46 ± 0.37	1.89 ± 0.42
Sharpness	1.01 ± 0.06	1.03 ± 0.11	1.16 ± 0.25	1.53 ± 0.33	1.97 ± 0.24	2.04 ± 0.25	2.31 ± 0.36	2.62 ± 0.37
Pelvis								
Artifact	1.10 ± 0.28	1.09 ± 0.27	1.09 ± 0.27	1.17 ± 0.30	2.08 ± 0.38	2.08 ± 0.37	2.09 ± 0.36	2.09 ± 0.36
Noise	1.10 ± 0.22	1.18 ± 0.25	1.60 ± 0.48	2.09 ± 0.36	1.09 ± 0.21	1.15 ± 0.27	1.41 ± 0.33	1.75 ± 0.35
Sharpness	1.04 ± 0.13	1.04 ± 0.14	1.14 ± 0.28	1.48 ± 0.33	1.87 ± 0.31	2.02 ± 0.28	2.24 ± 0.32	2.41 ± 0.35

Note.—Data are means ± standard deviations.

To clarify the influence of TOF on the image quality evaluation, we compared all PET_{TOF} with all $PET_{non\text{-}TOF}$ using the Wilcoxon signed-rank test with Bonferroni correction, where the P value was multiplied by 13.

The generalized estimating equation was applied for per-lesion analyses to test for clustering of lesions within patients. The effect of clustering was not significant ($P > .05$ for all) and therefore justified the assumption that all lesions could be analyzed independently.

$P < .05$ was considered to indicate a significant difference. Weighted κ was calculated by using R, and the other statistical analyses were performed with SPSS Statistics, version 19.0.0 (IBM, Armonk, NY).

Results

Overall, 74 patients were included consecutively without further selection (29 women, 45 men; median age, 63 years; range, 29–84 years) (Table 1). The median injected tracer activity was 219.5 MBq (range, 177.6–337.5 MBq), and the PET/CT acquisition was started a median of 72 minutes after the injection (range, 46–104 minutes). PET/MR imaging was performed after PET/CT in 36 patients and before PET/CT in 38 patients. The sequence of the PET/CT and PET/MR imaging examinations was determined in a random fashion, depending on the clinical workflow and the schedule for both systems. The PET/MR imaging system is located in an adjacent room next to the PET/CT room; thus, the time difference between the start of both acquisitions was 34 minutes ± 13 (range, 16–77 minutes). In five patients, $^{70\%}PET$ could not be reconstructed, and in two patients, $^{70\%}PET$ and $^{60\%}PET$ could not be reconstructed. This was due to a lower number of emitted counts in the PET/MR imaging examination (short scan duration at PET/MR and/or relatively long waiting time between PET/CT and PET/MR).

Agreement between Readers

The weighted κ between readers was moderate to substantial (image quality $[IQ]_{MIP}$, 0.60; $IQ_{artifact}$, 0.59; IQ_{noise}, 0.50; $IQ_{sharpness}$, 0.70; and IQ_{lesion}, 0.73).

Image Quality Analysis: Whole-Body and Body Part Compartments

IQ_{MIP} and $IQ_{artifact,\ noise,\ and\ sharpness}$ of $^{70\%}PET_{TOF}$ and $^{60\%}PET_{TOF}$ (from PET/MR imaging) were adequate for clinical imaging. In these two groups, all image quality scores were 2 or lower in 97% of patients (Table 3). The evaluated $^{60\%}PET_{non\text{-}TOF}$, $^{50\%}PET_{non\text{-}TOF}$, and $^{40\%}PET_{non\text{-}TOF}$ images were rated not adequate in all BMI groups. In these groups, more than two categories of image quality scores were higher than 2 in more than one-third of patients (Table 3). The evaluated $^{40\%}PET_{TOF}$ was partially not adequate either.

On the basis of these initial analyses, we performed further analysis in $^{50\%}PET_{TOF}$ and $^{70\%}PET_{non\text{-}TOF}$ by classifying them into the four BMI groups mentioned above. For the $^{50\%}PET_{TOF}$ subgroup, there were significant differences in several image quality evaluations among the four BMI groups (IQ_{MIP}, $IQ_{CH\_sharpness}$, and IQ_{PE_noise}, $P < .05$; IQ_{CH_noise} and IQ_{UA_noise},

$P < .01$). In the group with BMIs of less than 20 kg/m^2 and the group with BMIs of 20–25 kg/m^2, IQ_{MIP} and $IQ_{artifact,\ noise,\ and\ sharpness}$ were adequate for clinical imaging, while in the group with BMIs of 25–30 kg/m^2 and the group with BMIs of greater than 30 kg/m^2, these scores were not adequate (Fig 2, Fig E1 [online]).

Figure 2

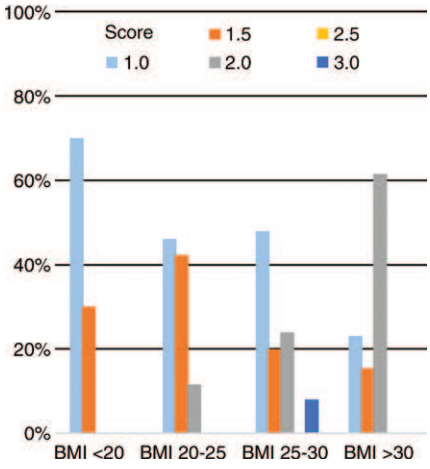

Figure 2: Bar chart shows percentage distribution of image quality of MIP images among four BMI groups in $^{50\%}PET_{TOF}$. Other representative categories are given in Figure E1 (online).

In $^{70\%}PET_{non\_TOF}$, there was no significant difference among all four BMI groups. However, in any of the BMI groups, the results of artifact and sharpness evaluation were found to be not fully adequate for clinical imaging. Particularly in $IQ_{CH\_sharpness}$, $IQ_{UA\_sharpness}$, and $IQ_{PE\_artifact}$, the average scores were approximately 2 and partly above 2 (Table 4). Images from a representative examination are shown in Figure 3. More detailed results of image quality scores are given in Tables E1–E4 (online).

Effect of TOF on Image Quality

The $^{70\%}PET_{non\text{-}TOF}$ images were significantly inferior to all TOF images with regard to artifacts and sharpness. However, in IQ_{MIP}, IQ_{HN_noise}, IQ_{CH_noise}, and IQ_{UA_noise}, $^{70\%}PET_{non\text{-}TOF}$ was superior to $^{50\%}PET_{TOF}$ and $^{40\%}PET_{TOF}$. In $IQ_{PE\_noise,}$ $^{70\%}PET_{non\text{-}TOF}$ was superior to $^{60\%}PET_{TOF}$, $^{50\%}PET_{TOF}$, and $^{40\%}PET_{TOF}$ (Table 5).

Lesion Conspicuity

PET_{TOF} was significantly superior to PET_{non_TOF}, even when we compared $^{40\%}PET_{TOF}$ with $^{70\%}PET_{non\_TOF}$ (1.53 ± 0.70 vs 2.30 ± 1.00, $P < .01$) (Table 6). Although the category IQ_{lesion} of $^{40\%}PET_{TOF}$ had somewhat lower scores, no lesions were missed. In comparison, in PET_{non_TOF}, several lesions were not definitively detectable on the PET image (lesions were actually overlooked during the evaluation). In $^{40\%}PET_{non\_TOF}$, 12 lesions (8.7%; long-axis diameter, 10.8 mm ± 3.8; range, 5–21 mm) were not reliably detected by the readers. In 10 (83.3%) of these 12 patients, PET/MR imaging was performed after PET/CT (with the starting time difference in scans being 26 minutes ± 6; range, 22–41 minutes). Images from a representative examination are shown in Figure 4.

Discussion

In our study, several aspects concerning image quality of PET images with simulated reduced ^{18}F-FDG doses from

Table 4

Image Quality Scores of TOF-PET/MR Imaging with SiPM Detectors in Each BMI Group in 50% of Counts with TOF and 70% Counts without TOF (*n* = 74)

	$^{50\%}PET_{TOF}$				$^{70\%}PET_{non\text{-}TOF}$			
Parameter	BMI < 20 kg/m^2 (*n* = 10)	BMI 20–25 kg/m^2 (*n* = 26)	BMI 25–30 kg/m^2 (*n* = 25)	BMI > 30 kg/m^2 (*n* = 13)	BMI < 20 kg/m^2 (*n* = 10)	BMI 20–25 kg/m^2 (*n* = 26)	BMI 25–30 kg/m^2 (*n* = 25)	BMI > 30 kg/m^2 (*n* = 13)
Whole-body MIP	1.15 ± 0.23	1.33 ± 0.34	1.50 ± 0.60	1.69 ± 0.42	1.00 ± 0.00	1.00 ± 0.00	1.15 ± 0.34	1.00 ± 0.00
Body compartments								
Head and neck								
Artifact	1.45 ± 0.27	1.50 ± 0.34	1.48 ± 0.39	1.46 ± 0.41	1.72 ± 0.53	1.86 ± 0.48	1.76 ± 0.53	1.62 ± 0.40
Noise	1.20 ± 0.33	1.38 ± 0.35	1.26 ± 0.29	1.31 ± 0.37	1.00 ± 0.00	1.02 ± 0.10	1.02 ± 0.10	1.00 ± 0.00
Sharpness	1.05 ± 0.15	1.10 ± 0.20	1.04 ± 0.14	1.08 ± 0.18	1.72 ± 0.25	1.68 ± 0.32	1.54 ± 0.36	1.69 ± 0.31
Chest								
Artifact	1.10 ± 0.30	1.06 ± 0.21	1.04 ± 0.14	1.00 ± 0.00	1.50 ± 0.71	1.39 ± 0.56	1.52 ± 0.38	1.19 ± 0.24
Noise	1.20 ± 0.24	1.62 ± 0.37	1.86 ± 0.50	2.00 ± 0.20	1.00 ± 0.00	1.09 ± 0.24	1.22 ± 0.49	1.12 ± 0.21
Sharpness	1.00 ± 0.00	1.17 ± 0.24	1.34 ± 0.37	1.23 ± 0.42	1.94 ± 0.28	1.77 ± 0.25	2.00 ± 0.36	1.96 ± 0.13
Upper abdomen								
Artifact	1.10 ± 0.30	1.06 ± 0.21	1.04 ± 0.14	1.04 ± 0.13	1.67 ± 0.71	1.52 ± 0.57	1.54 ± 0.41	1.54 ± 0.36
Noise	1.25 ± 0.25	1.58 ± 0.41	1.60 ± 0.47	1.88 ± 0.40	1.06 ± 0.16	1.05 ± 0.21	1.13 ± 0.26	1.04 ± 0.13
Sharpness	1.15 ± 0.23	1.15 ± 0.27	1.16 ± 0.23	1.15 ± 0.23	1.94 ± 0.16	1.95 ± 0.26	1.96 ± 0.25	2.04 ± 0.24
Pelvis								
Artifact	1.15 ± 0.32	1.12 ± 0.32	1.04 ± 0.14	1.12 ± 0.29	2.22 ± 0.67	2.11 ± 0.37	2.00 ± 0.21	2.08 ± 0.33
Noise	1.30 ± 0.33	1.56 ± 0.45	1.60 ± 0.51	1.92 ± 0.38	1.06 ± 0.16	1.11 ± 0.21	1.11 ± 0.25	1.04 ± 0.13
Sharpness	1.00 ± 0.00	1.15 ± 0.30	1.10 ± 0.24	1.27 ± 0.32	1.83 ± 0.24	1.86 ± 0.31	1.87 ± 0.26	1.88 ± 0.40

Note.—Data are means ± standard deviations.

Figure 3

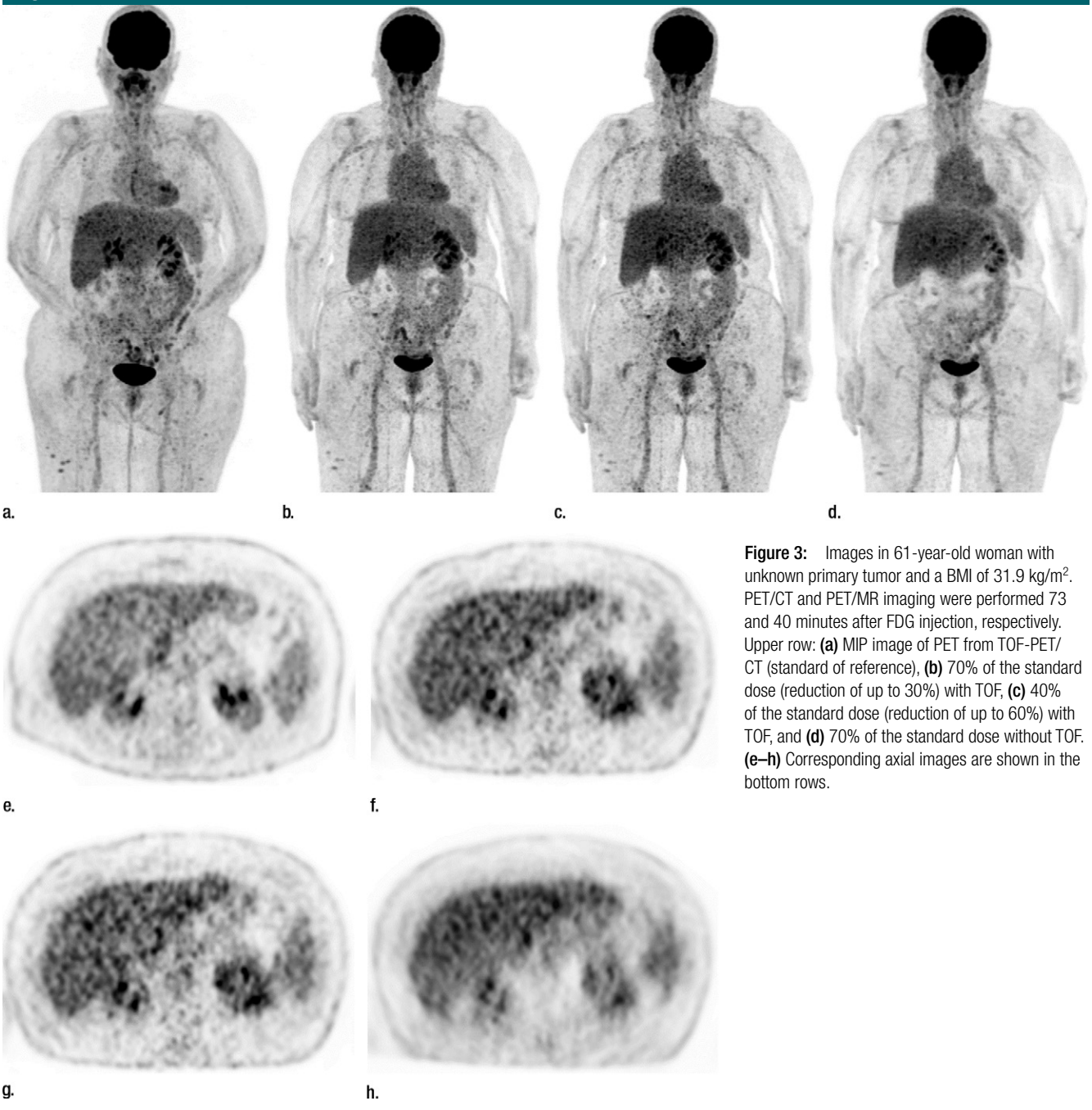

Figure 3: Images in 61-year-old woman with unknown primary tumor and a BMI of 31.9 kg/m^2. PET/CT and PET/MR imaging were performed 73 and 40 minutes after FDG injection, respectively. Upper row: **(a)** MIP image of PET from TOF-PET/CT (standard of reference), **(b)** 70% of the standard dose (reduction of up to 30%) with TOF, **(c)** 40% of the standard dose (reduction of up to 60%) with TOF, and **(d)** 70% of the standard dose without TOF. **(e–h)** Corresponding axial images are shown in the bottom rows.

a TOF-PET/MR imaging system were evaluated to find the lowest injectable dose of ^{18}F-FDG acceptable for routine clinical imaging.

Overall, image quality with simulated 60% of the standard injected dose of ^{18}F-FDG (reduction of up to 40%) was found to be clinically adequate. Furthermore, image quality with 50% of the simulated standard dose of injected ^{18}F-FDG (reduction of up to 50%) was comparable in patients with low or normal BMIs (BMI < 25 kg/m^2). Using TOF reconstruction improved the image quality, especially in relation to artifacts and sharpness. No lesions were missed on dose-reduced images with TOF.

Our results revealed that simulated 60% of the standard dose for all patients, and simulated 50% of the

standard dose in patients with a medium to low BMI, can safely be applied in clinical PET/MR imaging. The results of our study therefore confirm an earlier, more preliminary study with a smaller number of patients ($n = 25$) and extends the results through the use of a more in-depth evaluation of several image quality parameters (5). Notably, lesion detection was not impaired even with simulated 40% of the standard dose. Although image quality was considerably decreased, no lesion was missed on the TOF images. This might offer the possibility of further dose reduction (eg, in younger patients when following up specific lesions is the main imaging indication).

Several parts of the presented results can be explained by the technology used. New detector material in conjunction with a larger FOV was used, which provides a significantly increased sensitivity (11). This effect has been proven for other PET/MR systems as well (9). To illustrate clinical practicability: In our center, a patient with a BMI of less than 25 kg/m^2 would currently be injected with 3 MBq of ^{18}F-FDG per kilogram of body weight for PET/CT (eg, 75 kg of body weight = 225 MBq of injected activity). Applying the results of our study, this patient would then be injected with approximately 112.5 MBq for PET/MR imaging, while the same acquisition time and adequate clinical image quality were maintained. With 185 MBq equaling an effective absorbed dose of around 3.5 mSv, 112.5 MBq would decrease the radiation burden to approximately 2.2 mSv for a whole-body PET examination (18). Other studies have already quantified the dose reduction that can be achieved with PET/MR imaging compared with PET/CT only by omitting the CT component (7). In this context, the PET component represents the more significant radiation burden and thus offers a greater potential for reduction of the injected tracer dose. Of note, these advantages were tested in our study only for body imaging, but not for brain imaging. Here, the advantages are presumably substantially smaller because of higher attenuation from the head and neck coil, as well as from the nonutilization of the whole FOV in brain imaging (19,20).

In patients with a BMI of greater than 25 kg/m^2, a simulated 50% of the standard injected dose was not considered clinically adequate by the readers. This can be explained by the fact that, as in PET/CT, the body habitus of larger patients causes more scatter in the images. The TOF component partly resolves these issues, and the extent of improvement compared with thenon-TOF images can be appreciated

Table 5

Comparison of $^{70\%}PET_{non\_TOF}$ with $^{70\%}PET_{TOF}$, $^{60\%}PET_{TOF}$, $^{50\%}PET_{TOF}$, $^{40\%}PET_{TOF}$ of TOF-PET/MR Imaging with SiPM Detectors ($n = 74$)

$^{70\%}PET_{non\_TOF}$	$^{70\%}PET_{TOF}$	$^{60\%}PET_{TOF}$	$^{50\%}PET_{TOF}$	$^{40\%}PET_{TOF}$
Whole-body MIP	Nonsignificant	Nonsignificant	Superior	Superior
Each body part				
Head and neck				
Artifact	Inferior	Inferior	Inferior	Inferior
Noise	Nonsignificant	Nonsignificant	Superior	Superior*
Sharpness	Inferior	Inferior	Inferior	Inferior
Chest				
Artifact	Inferior	Inferior	Inferior	Inferior
Noise	Nonsignificant	Nonsignificant	Superior	Superior
Sharpness	Inferior	Inferior	Inferior	Inferior
Upper abdomen				
Artifact	Inferior	Inferior	Inferior	Inferior
Noise	Nonsignificant	Nonsignificant	Superior	Superior
Sharpness	Inferior	Inferior	Inferior	Inferior
Pelvis				
Artifact	Inferior	Inferior	Inferior	Inferior
Noise	Nonsignificant	Superior*	Superior	Superior
Sharpness	Inferior	Inferior	Inferior	Inferior

Note.—All "superior" or "inferior" differences were statistically confirmed with $P < .01$.

* $P < .05$.

Table 6

Evaluation of Malignant Lesions at TOF-PET/MR Imaging with SiPM Detectors ($n = 138$)

	TOF = On				TOF = Off			
Parameter	$^{70\%}PET_{TOF}$	$^{60\%}PET_{TOF}$	$^{50\%}PET_{TOF}$	$^{40\%}PET_{TOF}$	$^{70\%}PET_{non\text{-}TOF}$	$^{60\%}PET_{non\text{-}TOF}$	$^{50\%}PET_{non\text{-}TOF}$	$^{40\%}PET_{non\text{-}TOF}$
Score*	1.23 ± 0.47	1.26 ± 0.51	1.35 ± 0.59	1.53 ± 0.70	2.30 ± 1.00	2.39 ± 1.00	2.54 ± 1.09	2.75 ± 1.17
Score > 2.0	5 (3.6)	5 (3.6)	9 (6.5)	17 (12.3)	50 (36.2)	59 (42.8)	64 (46.4)	83 (60.1)
Lesion not detected	0	0	0	0	3 (2.2)	3 (2.2)	7 (5.1)	12 (8.7)

Note.—Unless otherwise specified, data are numbers of lesions, with percentages in parentheses.

* Data are means ± standard deviations.

Figure 4

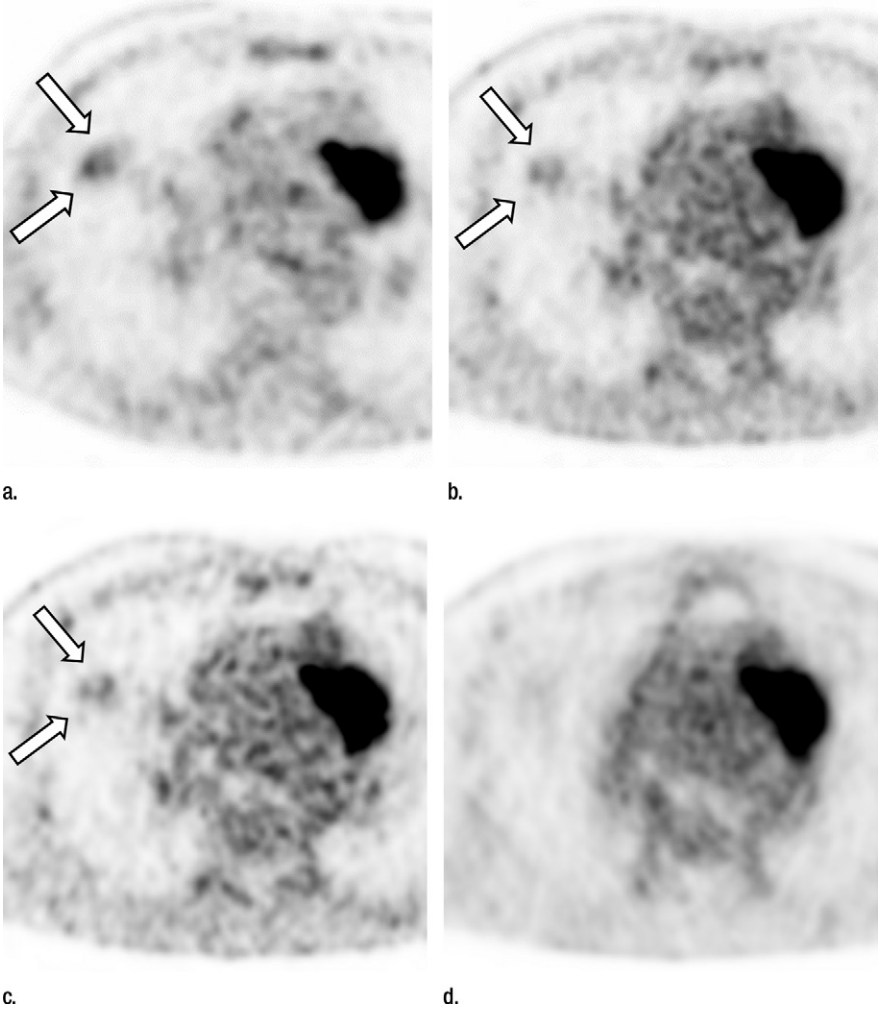

Figure 4: Images in 67-year-old man with lung cancer (arrows). **(a)** Axial PET image from TOF-PET/CT (standard of reference), **(b)** 70% of the standard dose (reduction of up to 30%) with TOF, **(c)** 40% of the standard dose (reduction of up to 60%) with TOF, and **(d)** 70% of the standard dose without TOF are shown. PET/CT and PET/MR were performed 94 and 58 minutes after FDG injection, respectively. On **c**, the PET image with 40% of the dose, the tumor (arrows) is visible, whereas on **d**, the non-TOF PET image with 70% of the standard dose, the tumor is no longer detectable.

in our results and has already been reported (21). However, this technique has its limitations, too. Thus, in very large patients, if the same amount of injected dose reduction is desired, the scan time per bed position might be prolonged to achieve good diagnostic quality.

There were some discrepancies between the IQ_{MIP} and the image quality for several body compartments and the IQ_{lesion} results. The $^{70\%}PET_{non\text{-}TOF}$ was found to be superior compared with $^{50\%}PET_{TOF}$ and $^{40\%}PET_{TOF}$ concerning noise. In contrast, IQ_{lesion} of $^{70\%}PET_{non\text{-}TOF}$ was found to be significantly inferior compared with $^{40\%}PET_{TOF}$; therefore, artifacts and/or sharpness—rather than noise—seem to be at least equally important parameters concerning lesion conspicuity and detectability.

However, care should be taken regarding in which organ or body compartment lesions are located. For example, images of the liver usually have a high degree of noise, and this certainly impairs lesion detection more than in the lung, for example. Furthermore, the conspicuity and detectability of the tumor partly also depend on the postinjection time. A later scan could potentially provide a higher contrast-to-noise ratio in malignant lesions (22). In our study, 10 of 12 lesions missed at $^{40\%}PET_{non\text{-}TOF}$ were imaged before PET/CT. Hence, the contrast-to-noise ratio in these images might have been lower than in the reference image. However, the order of the scanning times between PET/CT and PET/MR imaging was randomly based on the clinical workflow and availability of the scanners. Furthermore, because both systems are located in two rooms directly adjacent to each other, the difference in acquisition start time between both acquisitions was not significantly different.

Our study had several limitations. First, the resolution of the images was inherently different between PET/CT and PET/MR imaging. However, there is no effective technical method (at least no way that would not outstrip the focus of our study) to equalize both resolutions. In addition, several other factors (eg, uptake time, attenuation correction method) can affect the PET image quality and appearance in patient studies (23). Because we mainly made qualitative comparisons, those differences were partly compensated for and are largely negligible for the purpose of our study, given the setup we used (eg, a very low time difference between PET/CT and PET/MR imaging). Subsets and iterations between TOF-PET/CT and TOF-PET/MR imaging were based on our routine clinical experience and the pertinent literature (11). However, these parameters were not additionally optimized for non-TOF reconstruction at PET/MR imaging. Other publications (12,24) have already shown that the differences for such comparisons are negligible.

In conclusion, a simulated 60% of the injected standard dose (reduction of up to 40%) of ^{18}F-FDG in patients with a BMI greater than 25 kg/m^2 still results in clinically adequate PET image quality at TOF-PET/MR imaging. Additionally, in patients with a BMI of less than 25 kg/

m^2, 50% of the injected standard dose (reduction of up to 50%) can be safely applied as well. Thus, substantially lower radiation dose compared with those at conventional PET/CT can be achieved in PET/MR imaging with SiPM detectors—not only by omitting the CT component, but also by optimizing use of the PET component.

Disclosures of Conflicts of Interest: T.S. disclosed no relevant relationships. **G.D.** Activities related to the present article: is an employee of GE Healthcare. Activities not related to the present article: disclosed no relevant relationships. Other relationships: disclosed no relevant relationships. **K.G.Z.** disclosed no relevant relationships. **F.d.G.B.** disclosed no relevant relationships. **E.E.G.W.t.V.** disclosed no relevant relationships. **M.H.** Activities related to the present article: disclosed no relevant relationships. Activities not related to the present article: institution has received grants from GE Healthcare; is on the speakers bureau of GE Healthcare. Other relationships: disclosed no relevant relationships. **P.V.** Activities related to the present article: GE Healthcare grant to institution covered research of which the current article is a part. Activities not related to the present article: institution received grants from GE Healthcare and Roche Pharmaceuticals; institution received supplies of contrast media from Bayer Healthcare. Other relationships: disclosed no relevant relationships.

References

1. Radford J, Illidge T, Counsell N, et al. Results of a trial of PET-directed therapy for early-stage Hodgkin's lymphoma. N Engl J Med 2015;372(17):1598–1607.
2. Fischer B, Lassen U, Mortensen J, et al. Preoperative staging of lung cancer with combined PET-CT. N Engl J Med 2009; 361(1):32–39.
3. Boellaard R, Delgado-Bolton R, Oyen WJ, et al. FDG PET/CT: EANM procedure guidelines for tumour imaging: version 2.0. Eur J Nucl Med Mol Imaging 2015;42(2):328–354.
4. Karakatsanis NA, Fokou E, Tsoumpas C. Dosage optimization in positron emission tomography: state-of-the-art methods and future prospects. Am J Nucl Med Mol Imaging 2015;5(5):527–547.
5. Queiroz MA, Delso G, Wollenweber S, et al. Dose optimization in TOF-PET/MR compared to TOF-PET/CT. PLoS One 2015;10(7): e0128842.
6. Zeimpekis KG, Barbosa F, Hüllner M, et al. Clinical evaluation of PET image quality as a function of acquisition time in a new TOF-PET/MRI compared to TOF-PET/CT--initial results. Mol Imaging Biol 2015;17(5):735–744.
7. Melsaether AN, Raad RA, Pujara AC, et al. Comparison of whole-body (18)F FDG PET/MR imaging and whole-body (18)F FDG PET/CT in terms of lesion detection and radiation dose in patients with breast cancer. Radiology 2016;281(1):193–202.
8. Levin C, Deller T, Peterson W, Maramraju SH, Kim C, Prost R. Initial results of simultaneous whole-body ToF PET/MR [abstr]. J Nucl Med 2014;55(Suppl 1):660.
9. Delso G, Fürst S, Jakoby B, et al. Performance measurements of the Siemens mMR integrated whole-body PET/MR scanner. J Nucl Med 2011;52(12):1914–1922.
10. Boellaard R, Quick HH. Current image acquisition options in PET/MR. Semin Nucl Med 2015;45(3):192–200.
11. Bettinardi V, Presotto L, Rapisarda E, Picchio M, Gianolli L, Gilardi MC. Physical performance of the new hybrid PET/CT Discovery-690. Med Phys 2011;38(10):5394–5411.
12. Davison H, ter Voert EE, de Galiza Barbosa F, Veit-Haibach P, Delso G. Incorporation of time-of-flight information reduces metal artifacts in simultaneous positron emission tomography/magnetic resonance imaging: a simulation study. Invest Radiol 2015;50(7):423–429.
13. Wollenweber S, Ambwani S, Lonn A, et al. Comparison of 4-class and continuous fat/water methods for whole-body, MR-based PET attenuation correction. Nuclear Science Symposium and Medical Imaging Conference (NSS/MIC), 2012 IEEE. Piscataway, NJ: IEEE, 2012; 3019–3025.
14. Masuda Y, Kondo C, Matsuo Y, Uetani M, Kusakabe K. Comparison of imaging protocols for 18F-FDG PET/CT in overweight patients: optimizing scan duration versus administered dose. J Nucl Med 2009;50(6):844–848.
15. Watson CC, Casey ME, Bendriem B, et al. Optimizing injected dose in clinical PET by accurately modeling the counting-rate response functions specific to individual patient scans. J Nucl Med 2005;46(11):1825–1834.
16. Oehmigen M, Ziegler S, Jakoby BW, Georgi JC, Paulus DH, Quick HH. Radiotracer dose reduction in integrated PET/MR: implications from national electrical manufacturers association phantom studies. J Nucl Med 2014;55(8):1361–1367.
17. Landis JR, Koch GG. The measurement of observer agreement for categorical data. Biometrics 1977;33(1):159–174.
18. Boellaard R, O'Doherty MJ, Weber WA, et al. FDG PET and PET/CT: EANM procedure guidelines for tumour PET imaging: version 1.0. Eur J Nucl Med Mol Imaging 2010;37(1):181–200.
19. Wollenweber SD, Delso G, Deller T, Goldhaber D, Hüllner M, Veit-Haibach P. Characterization of the impact to PET quantification and image quality of an anterior array surface coil for PET/MR imaging. MAGMA 2014;27(2):149–159.
20. Sekine T, Burgos N, Warnock G, et al. Multi-atlas-based attenuation correction for brain 18F-FDG PET imaging using a time-of-flight PET/MR scanner: comparison with clinical single-atlas- and CT-based attenuation correction. J Nucl Med 2016;57(8): 1258–1264.
21. Vandenberghe S, Mikhaylova E, D'Hoe E, Mollet P, Karp JS. Recent developments in time-of-flight PET. EJNMMI Phys 2016; 3(1):3.
22. Laffon E, Adhoute X, de Clermont H, Marthan R. Is liver SUV stable over time in ^{18}F-FDG PET imaging? J Nucl Med Technol 2011;39(4):258–263.
23. Boellaard R. Standards for PET image acquisition and quantitative data analysis. J Nucl Med 2009;50(Suppl 1):11S–20S.
24. de Galiza Barbosa F, Delso G, Zeimpekis KG, et al. Evaluation and clinical quantification of neoplastic lesions and physiological structures in TOF-PET/MRI and non-TOF/MRI - a pilot study. Q J Nucl Med Mol Imaging 2015 May 12. [Epub ahead of print]